LETTERS
PUBLISHED ONLINE: 16 MAY 2010 | DOI: 10.1038/NGEO856
nature geoscience

Magnitude of oceanic nitrogen fixation influenced by the nutrient uptake ratio of phytoplankton

Matthew M. Mills* and Kevin R. Arrigo

The elemental stoichiometry of sea water and particulate organic matter is remarkably similar. This observation led Redfield to hypothesize that the oceanic ratio of nitrate to phosphate is controlled by the remineralization of phytoplankton biomass[1]. The Redfield ratio is used universally to quantitatively link the marine nitrogen and phosphorus cycles in numerous biogeochemical applications[2–4]. Yet, empirical and theoretical studies show that the ratio of nitrogen to phosphorus in phytoplankton varies greatly with taxa[5,6] and growth conditions[7–9]. Here we present a dynamic five-box ecosystem model showing that non-Redfield utilization of dissolved nitrogen and phosphorus by non-nitrogen-fixing phytoplankton controls the magnitude and distribution of nitrogen fixation. In our simulations, systems dominated by rapidly growing phytoplankton with low nitrogen to phosphorus uptake ratios reduce the phosphorus available for nitrogen fixation. In contrast, in systems dominated by slow-growing phytoplankton with high nitrogen to phosphorus uptake ratios nitrogen deficits are enhanced, and nitrogen fixation is promoted. We show that estimates of nitrogen fixation are up to fourfold too high when non-Redfield uptake stoichiometries are ignored. We suggest that the relative abundance of fast- and slow-growing phytoplankton controls the amount of new nitrogen added to the ocean.

The notion of a constant nitrogen/phosphorus ratio for both phytoplankton and the deep ocean shapes our current understanding of the balance between nitrogen and phosphorus inventories in the ocean. In this framework, processes that remove oceanic fixed nitrogen (for example, denitrification) and drive the nitrate/phosphate ratio from the canonical Redfield ratio are approximately balanced by nitrogen inputs, primarily from nitrogen fixation[3,10]. However, field and laboratory data confirm that non-Redfield nutrient utilization is common in phytoplankton, with N/P utilization ratios being below Redfield during blooms[6,9] and above Redfield in oligotrophic regions dominated by cyanobacteria[8,9] (including non-diazotrophs). One explanation for this N/P plasticity is that fast-growing cells require abundant P-rich growth machinery and exhibit low cellular N/P ratios[7,9]. In contrast, resource-limited cells invest in N-rich light and/or nutrient acquisition machinery and have higher N/P ratios[7,9].

Despite the prevalence of non-Redfield nutrient utilization, few ecosystem models[11,12], and virtually no geochemical or ocean general circulation models that include biological processes, consider non-Redfield nutrient consumption, assuming instead that phytoplankton N/P stoichiometry is Redfield (diazotrophs notwithstanding). Considering the predominance of marine environments that support non-Redfield N/P utilization by non-diazotrophic phytoplankton, a better description of how phytoplankton stoichiometry affects oceanic nutrient inventories is critical to understanding the marine N cycle.

We developed a dynamic five-box ecosystem model (Fig. 1) with three phytoplankton groups (diatoms, picocyanobacteria and diazotrophs) to understand how changes in seawater NO_3/PO_4 stoichiometry, mediated by non-Redfield phytoplankton N/P requirements, influence N_2 fixation and, ultimately, the oceanic inventory of N in the eastern tropical South Pacific Ocean (ETSP). Briefly, the model includes flow between compartments representing the deep ocean, the nearshore subsurface oxygen minimum zone (OMZ) where fixed N is lost through microbial processes, the coastal upwelling zone dominated by diatoms[13,14] with low N/P requirements[5], transitional waters between the coastal upwelling and the oligotrophic ocean, and the oligotrophic gyre dominated by picocyanobacteria (for example, *Prochlorococcus*[15]) with high N/P requirements[8]. Changes in N and P inventories were simulated over an annual cycle in each box using different assumptions about phytoplankton N/P stoichiometry in each simulation. N_2 fixation was calculated from diazotroph growth and the fraction of the N requirement satisfied by N_2 fixation. We also calculated the amount of N_2 fixation required in each box to restore PO_4 concentrations to the observed World Ocean Atlas (WOA) 2005 climatology[16]. Results from the Redfield and non-Redfield simulations were then compared (for model details, see the Methods section).

In the coastal upwelling box, chlorophyll *a* (chl) varies seasonally from 0.5 to 2.0 mg m^{-3} (Supplementary Fig. S1) and is dominated by diatoms (89%; refs 13,14), with picocyanobacteria and diazotrophs making up 10% and 1% of the community, respectively. In the Redfield simulation, diazotrophs obtain 9–25% of their N from N_2 fixation, depending on seasonal variations in NO_3, and fix 1.5×10^9 mmol N yr^{-1}. Whereas seasonal NO_3 dynamics are consistent with the observed climatology, PO_4 is substantially too high, averaging 1.62 ± 0.09 mmol m^{-3} (Fig. 2a, Supplementary Table S2). The modelled NO_3/PO_4 ratio in the upwelling box is below Redfield because of input of NO_3-depleted waters from the OMZ, as documented throughout the ETSP (refs 3,10). However, the predicted amount of excess PO_4 ($xsPO_4 = PO_4 - NO_3/16$; ref. 10) is 30% higher than observed (Fig. 2b). Sensitivity analyses show that once waters upwell to the surface, $xsPO_4$ is determined primarily by the phytoplankton N/P ratio (r), being much less sensitive to other model parameters (Supplementary Tables S5–S7). Under the Redfield assumption, another 0.26 mmol PO_4 m^{-3} would need to be removed from the upwelling box to bring modelled nutrient inventories into agreement with observed climatologies. This could be achieved only by allowing diazotrophs to consume >25% of the total available PO_4 and fix >13 mmol N m^{-3}, values that far exceed *in situ* observations in upwelling waters[17].

Community composition is similar in the upwelling and transitional boxes, with diatoms, picocyanobacteria and diazotrophs accounting for 85, 10 and 5%, respectively, of the

Department of Environmental Earth System Science, Stanford University, Stanford, California 94305, USA. *e-mail: mmmills@stanford.edu.

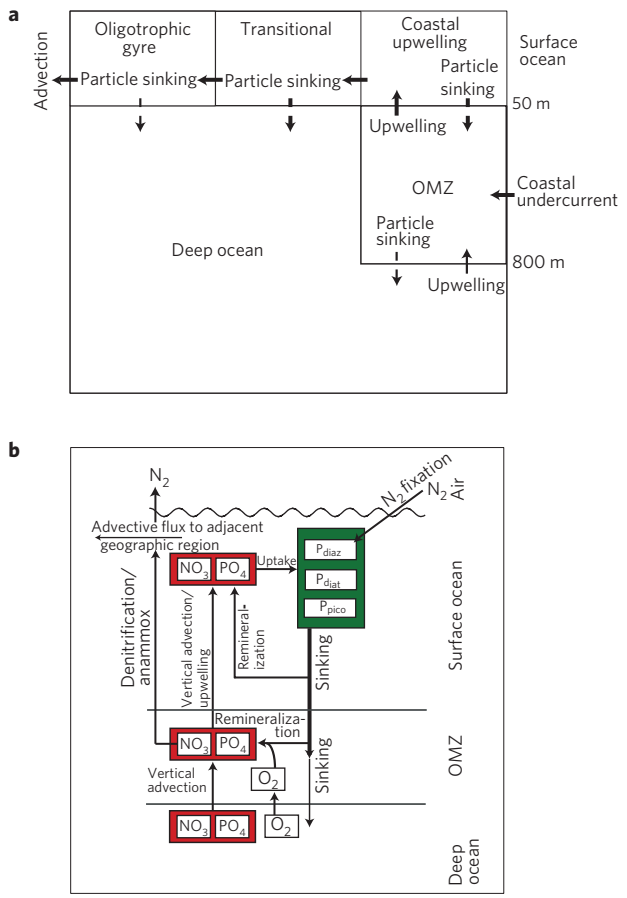

Figure 1 | The ETSP five-box ecosystem model. a, Diagram showing the flows between the different ocean boxes (denoted by solid arrows). The difference between deep flows into the OMZ and out to the coastal upwelling box is equal to the advection of suboxic coastal undercurrent water into the OMZ (Supplementary Table S1). Sinking particulates from the transitional and oligotrophic boxes do not alter nutrient concentrations in the much larger deep ocean box. **b**, Schematic representation of the biological model showing the relationship between state variables and the principal fluxes. Nutrients upwell only into the coastal box.

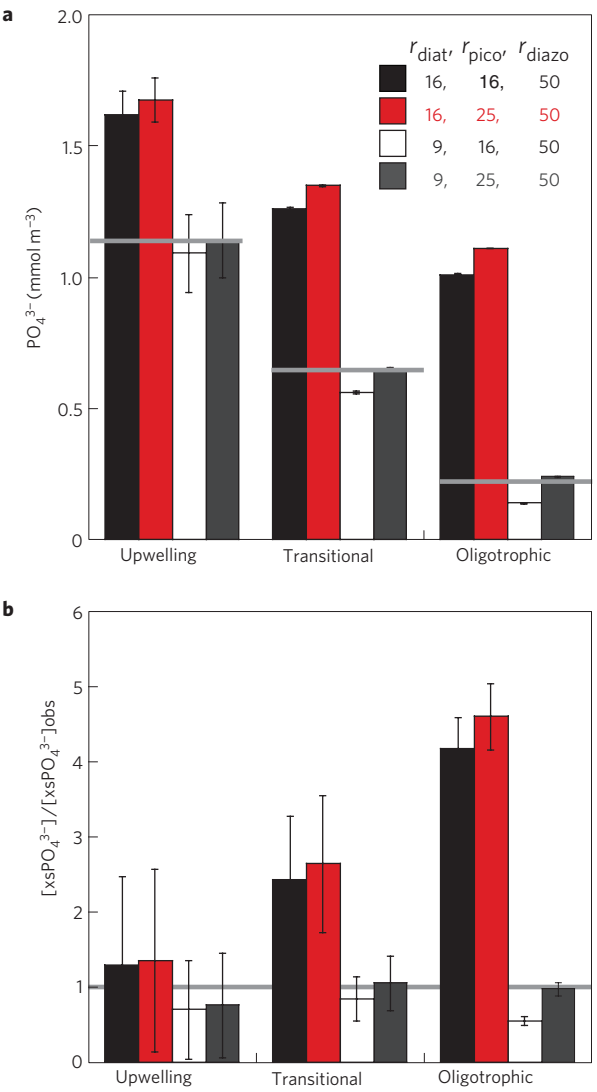

Figure 2 | Effects of phytoplankton nitrate/phosphate (NO_3/PO_4) utilization ratios on PO_4 and $xsPO_4$ in the ETSP. a,**b** Mean annual values ±s.d. for PO_4 concentrations (mmol m^{-3}) (**a**) and the ratio of modelled $xsPO_4$ to observed $xsPO_4$ (from the WOA2005; ref. 14) (**b**) for the three surface boxes using different elemental ratios (r_j). The grey lines in **a** represent observed annual means from the WOA2005 and the grey line in **b** represents perfect agreement between the modelled and observed $xsPO_4$ concentrations. The associated standard deviations of NO_3 and PO_4 used in the calculation of $xsPO_4$ are propagated as $s.d._{xsPO_4} = \sqrt{(s.d._{NO_3})^2 + (s.d._{PO_4})^2}$.

total chl pool. However, phytoplankton abundance is lower in this box and the annual cycle is dampened (0.15–0.23 mg chl m^{-3}, Supplementary Fig. S1). In the Redfield simulation, NO_3 agrees well with observations, but modelled PO_4 (1.26 ± 0.004 mmol m^{-3}) is about twofold too high (0.64 ± 0.28 mmol m^{-3}), requiring removal of a further 0.63 mmol P m^{-3} to reproduce observed concentrations in the ETSP (Fig. 2a, Supplementary Table S2). Depletion of this residual PO_4 pool requires that diazotrophs remove >80% of the total PO_4 and fix ~31 mmol N m^{-3}, rates far in excess of those documented in surface *Trichodesmium* blooms[18].

In the oligotrophic box, chl is low (0.05–0.07 mg m^{-3}, Supplementary Fig. S1) and dominated by picocyanobacteria (55%), with diatoms and diazotrophs comprising the remaining 35% and 10% of phytoplankton biomass, respectively[15]. In the Redfield simulation, nutrient assimilation yields reasonable levels of NO_3, whereas PO_4 concentrations are fourfold higher than observed (Fig. 2a and Supplementary Table S2). As a result of the low NO_3 concentrations in this box, the annual N_2-fixation rate of 12.6×10^9 mmol yr^{-1} provides >98% of the N for diazotrophs. However, diazotrophs would need to fix 38 mmol N m^{-3} and remove an extra 0.76 mmol PO_4 m^{-3} for the Redfield model to match observed nutrient inventories in oligotrophic waters. This is greater than the observed removal of PO_4 between the transitional and oligotrophic zones by all phytoplankton groups combined (Supplementary Table S2) and is therefore not tenable.

In the non-Redfield simulation, calculated NO_3 in each box was the same as in the Redfield simulation (Supplementary Table S5). However, PO_4 was substantially reduced and in much better agreement with climatology[16] throughout the ETSP (Fig. 2a, Supplementary Table S2). Enhanced PO_4 consumption by diatoms (owing to their low N/P ratio), particularly in the upwelling and transitional boxes, reduced the $xsPO_4$ (Fig. 2b) available to diazotrophs and resulted in markedly lower N_2-fixation rates compared with the Redfield simulation (Table 1). This was partially offset by higher than Redfield NO_3/PO_4 consumption by picocyanobacteria in the transitional and oligotrophic boxes,

Table 1 | Comparison of N_2-fixation rates in the three oceanographic regions under the different N/P utilization scenarios and assuming that diazotroph consumption returns $xsPO_4$ concentrations to observed climatology.

Oceanographic region		Area (10^8 m^2)	N_2-fixation rate (10^9 mmol yr^{-1}) N/P = 9, 25, 50*	16, 16, 50*	16, 25, 50*	9, 16, 50*
Box 3	Upwelling	0.22	1.5	2.1	2.1	1.4
Box 4	Transitional	1.07	7.2	14.0	15.0	6.2
Box 5	Oligotrophic	1.59	12.6	53.0	58.4	7.3
	Total	2.88	21.3	69.1	75.5	14.9
	Mean ± s.d.		7.1±5.6	23.0±26.7	25.2±29.5	5.0±3.1
	Relative to N/P = 9, 25, 50		1.0	3.3	3.6	0.7

*Diatom, picocyanobacteria and diazotroph N/P utilization ratios, respectively.

which slightly increased PO_4 concentrations (Fig. 2a) and N_2 fixation when r_{Pico} was increased from 16 to 25 (Table 1). However, because of diatom dominance, especially in the upwelling box, the net impact of non-Redfield nutrient stoichiometry was to reduce the $xsPO_4$ (Fig. 2b) available for N_2 fixation downstream. Consequently, in the upwelling box, N_2-fixation rates were 1.5-fold higher in the Redfield simulation than in the non-Redfield run (Table 1). The difference between the two simulations was even larger in the transitional box (twofold higher in the Redfield run) and culminated in N_2-fixation rates in the oligotrophic box that were fourfold higher in the Redfield run than in the non-Redfield simulation. Assumption of non-Redfield nutrient utilization in the ETSP leads to N_2-fixation rates that, although threefold lower than when Redfield stoichiometry is assumed (Table 1), are in agreement with estimates for the equatorial Pacific[4].

These results show that the relative diatom and picocyanobacteria abundance substantially impacts the amount of $xsPO_4$ available for diazotrophy. As diatoms dominate upwelling and transitional zones, they exert greater control on PO_4 availability than picocyanobacteria. As a consequence of lower diatom N/P requirements, the $xsPO_4$ in the upwelling box is reduced by 65% before reaching the oligotrophic box. Our results also clearly demonstrate the importance of considering actual nutrient utilization ratios when calculating N_2-fixation rates from nutrient inventories[3,10]. This is particularly relevant to productive waters overlying OMZs, such as the coastal waters that upwell off Peru, where observed nutrient ratios show $xsPO_4$ consumption (ref. 10; Supplementary Table S2). The assumption that NO_3/PO_4 utilization is Redfield in the ETSP probably leads to estimates of N_2 fixation that are up to fourfold too high (Table 1).

Our model, although reasonably mechanistic, makes some important simplifying assumptions, including holding both N/P utilization ratios and phytoplankton community composition fixed over time. Nevertheless, our results changed little when phytoplankton N/P requirements were allowed to vary seasonally (lower during exponential growth and higher at the end of the bloom). This is because the ratios used in the non-Redfield simulations are applicable during the exponential phase of blooms when most nutrients are removed. After the bloom, nutrient utilization ratios may be higher, but nutrient uptake is small, minimizing its impact. Similarly, allowing taxonomic composition to vary seasonally had little effect on $xsPO_4$ because only the minor taxa in each box were impacted by this assumption.

Recent studies suggest that the low NO_3/PO_4 ratio of waters that upwell to the surface from suboxic zones stimulates diazotrophy in areas proximal to OMZs, producing a tight spatial coupling between sources and sinks of oceanic fixed N (ref. 10). Tight coupling is predicted to lead to even greater denitrification rates as more organic matter produced through N_2 fixation is exported to depth, resulting in a runaway denitrification/N_2-fixation feedback loop[19]. Models can spatially decouple N_2 fixation and N loss by making diazotrophy inversely proportional to NO_3 availability or by allowing diatoms to outcompete diazotrophs when NO_3 concentrations are high. However, this decoupling does nothing to alter the $xsPO_4$ inventory when Redfield stoichiometry is invoked. Therefore, previous model-based estimates of areal N_2-fixation rates are 1–9-fold higher than those calculated here[20,21]. We note that our estimates are conservative and do not include N_2 fixation in the absence of cell growth[22]. Nevertheless, our analysis suggests that by reducing N_2-fixation rates within both upwelling and transitional zones, non-Redfield nutrient utilization by phytoplankton provides an effective mechanism to spatially decouple areas of N_2 fixation and N loss.

Non-Redfield nutrient utilization by non-diazotrophs may also be responsible for the observed patterns of $xsPO_4$ in the North Atlantic. $xsPO_4$ in waters from the Arctic Ocean[23] is reduced significantly during the massive phytoplankton blooms in the North Atlantic (Fig. 3a–h). These blooms are dominated by diatoms and coccolithophores[24] with low NO_3/PO_4 utilization ratios[5]. As they are located north of regions with substantial N_2 fixation[25], the seasonal reduction in $xsPO_4$ in these waters is best explained by phytoplankton nutrient drawdown at N/P ratios below Redfield. As in the ETSP, these fast-growing phytoplankton reduce the availability of PO_4 to diazotrophs in the North Atlantic, and thus, significantly diminish potential N_2-fixation rates.

Furthermore, nutrient utilization above Redfield by non-diazotrophs may contribute to the high excess NO_3 ($xsNO_3$, relative to Redfield proportions) in the subsurface North Atlantic subtropical gyre[3]. The overwhelmingly dominant autotrophs in these waters (*Prochlorococcus* and *Synechococcus*) have high cellular N/P quotas, and their contribution to export in oligotrophic environments may be significant[26]. The export and remineralization of this N-rich organic matter probably contribute to elevated $xsNO_3$ in subsurface waters and should be accounted for when using $xsNO_3$ to determine basin-scale N_2 fixation[3]. By similar reasoning, denitrification rates in OMZs that are calculated assuming sinking particulate matter is in Redfield proportions are probably overestimated by an amount proportional to the sinking flux and subsequent remineralization of low-N/P particulate organic matter originating at the surface.

Finally, the results presented here have important implications for understanding controls on global marine N inventories. Current views hold that N_2 fixation increases the N content of the predominantly N-limited oceans, stimulating organic matter production and export, reducing oxygen concentrations in the ocean interior and enhancing the loss of fixed N from the ocean through denitrification and anaerobic ammonium oxidation (anammox). We suggest that the relative abundance of phytoplankton with non-Redfield N/P requirements exerts significant control on the strength of this feedback. Contemporary phytoplankton distributions are such that slow-growing picocyanobacteria dominate oceanic gyres, whereas fast-growing taxa such as diatoms dominate high-nutrient environments such as upwelling waters overlying OMZs. Environmental changes that enhance ocean

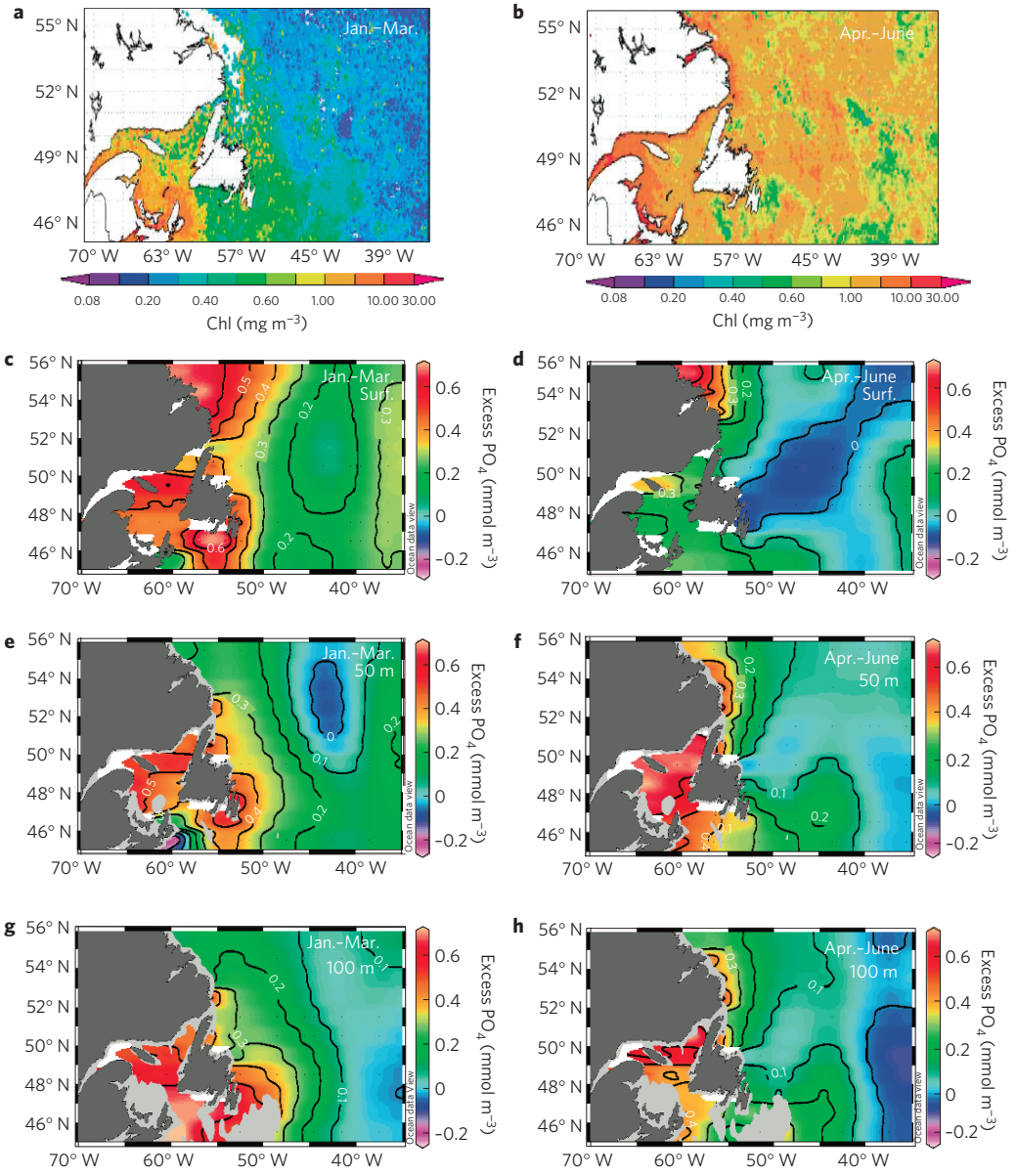

Figure 3 | Seasonal variation in excess PO_4 ($xsPO_4$, mmol m^{-3}) and chlorophyll (chl, mg m^{-3}) in the northern North Atlantic Ocean. a–h, Surface chl (**a**,**b**) and $xsPO_4$ at depths of 0 m (**c**,**d**), 50 m (**e**,**f**) and 100 m (**g**,**h**) for January–March (**a**,**c**,**e**,**g**) and April–June (**b**,**d**,**f**,**h**). Although wintertime nutrient data are relatively sparse (Supplementary Fig. S4), the seasonal decrease in $xsPO_4$ in the upper 100 m correlates with the spring diatom blooms in waters north of 40° N where diazotrophs are not typically found. Nutrients, from the WOA2005, are plotted using ODV (http://www.awi-bremerhaven.de/GEO/ODV). Chl was determined using the Giovanni Ocean Colour Time-Series Online Visualization software (http://odv.awi.de/).

stratification[27] will probably increase the area of the ocean's surface that is depleted in macronutrients, thereby expanding the habitat of high-N/P-using picocyanobacteria[28]. In contrast, perturbations that increase upwelling (for example, increased winds) will expand the habitat of diatoms having lower N/P ratios. The relative magnitude of these two changes could significantly impact $xsPO_4$ availability for diazotrophs, and hence the amount of new N added to the ocean through N_2 fixation. Therefore, the prevailing paradigm that the marine N inventory is controlled by a simple feedback between global rates of denitrification/anammox and N_2 fixation needs to be modified. Our results indicate that non-Redfield nutrient utilization by non-diazotrophic phytoplankton represents a mechanism that can decouple the processes of N_2 fixation and denitrification, and consequently, the steady-state oceanic N inventory. Furthermore, the reduction in $xsPO_4$ by diatoms and the corresponding decrease in downstream N_2 fixation may help explain the apparent imbalance between rates of N_2 fixation and fixed-N loss (which is substantially larger)[29] in the contemporary ocean.

Methods

In the model, water from the OMZ upwells into the surface coastal box with a low NO_3/PO_4 ratio. We model this input of nutrients as a product of the time-varying advective volume flux (f) and the associated nutrient concentration. Net growth of each phytoplankton group in the surface coastal box is determined from observed changes in chlorophyll a concentrations (from SeaWiFS) (Supplementary Fig. S1) and the proportion that each phytoplankton group contributes to the total phytoplankton population (as determined from published data). This net growth rate for each phytoplankton group is used to calculate uptake of nutrients at the specified utilization ratios. The NO_3/PO_4 utilization ratios (r) for diatoms, picocyanobacteria and diazotrophs are specified to be 16 (r_{diat}), 16 (r_{pico}) and 50 (r_{diazo}), respectively, in the 'Redfield' simulation. In the non-Redfield simulation, NO_3/PO_4 utilization ratios by diatoms ($r_{diat} = 9$) and picocyanobacteria ($r_{pico} = 25$) are altered to better conform with our improved understanding of phytoplankton stoichiometry[5,7,8]. A fraction of the newly formed particulate material (N or P) is remineralized within the surface box and the remainder either sinks below the

surface or advects into the transitional box. This information is used to calculate the inventories of NO_3 and PO_4 over an annual cycle within the box. This scheme is repeated when estimating the nutrient inventories for the transitional box and the oligotrophic box. Although variable surface water remineralization ratios may alter surface nutrient ratios[30], we suggest variability in this ratio is small. Finally, mass is conserved in the model by running it to a long-term steady state, at which point all N inputs equal N outputs.

Model details. As shown in Supplementary Equation (1) (Supplementary Table S3), all state variables in the model ($X = NO_3, PO_4, O_2$, or one of the three phytoplankton taxa, P_j, where j = diatoms, picocyanobacteria or diazotrophs) are impacted by both physical (f = advection and mixing) and biological (Q = nutrient uptake, remineralization and sinking) processes. Mixing between the subsurface OMZ box and the surface coastal box is calculated as a function of wind speed (Supplementary Information), as is advection between the surface coastal box, the transition zone box and the oligotrophic box.

The rate of change in phytoplankton biomass (mg N m^{-3} d^{-1}, Supplementary Equation (2)) in each box is calculated as a function of the phytoplankton growth rate (μ_j, d^{-1}), the daily fraction of P_j that is remineralized within each box (E_j, d^{-1}) and the daily fraction of P_j that sinks out of each box (s_j, d^{-1}). Changes in NO_3 and PO_4 concentration (mg m^{-3}, Supplementary Equations (3a) and (4a), respectively) are calculated as a function of phytoplankton uptake during growth (μ_j) and the remineralization of dead or grazed phytoplankton biomass (E_j, d^{-1}). The currency of the model is N, so changes in PO_4 (Supplementary Equation (4)) are coupled to those of NO_3 (Equation (3)) through the elemental N/P ratio of each phytoplankton taxa (r_j). As Supplementary Equations (3a) and (4a) require knowledge of $\mu_j P_j$ and $E_j P_j$ for each phytoplankton taxa, quantities that are not easily determined, we rearranged Supplementary Equation (2a) to take the form shown in Supplementary Equation (2b). Then we substituted the right side of Supplementary Equation (2b) for the left side and inserted it into Supplementary Equations (3a) and (4a) to yield Supplementary Equations (3b) and (4b), respectively. Supplementary Equations (3b) and (4b) are preferable to Supplementary Equations (3a) and (4a) because they rely only on changes in phytoplankton biomass, which can be derived from SeaWiFS, and phytoplankton sinking rate, a quantity that can be constrained easily using O_2 data and to which model results are relatively insensitive.

As formulated, Supplementary Equation (3a) assumes that all phytoplankton growth is supported by dissolved NO_3. However, this is not the case for diazotrophs, which use N_2 when NO_3 is low. We account for this in the second line of Supplementary Equation (3b), where κ_{N2} is the fraction of diazotroph N that comes from N_2 fixation (Supplementary Fig. S2). The instantaneous N_2-fixation rate (ρ) is then calculated in Supplementary Equation (6).

Finally, the rate of remineralization of sinking phytoplankton organic matter in the OMZ is constrained using observed O_2/P remineralization ratios[2] such that modelled O_2 concentrations are consistent with the WOA climatology. Changes in O_2 concentration in the model are calculated as in Supplementary Equation (7), where E_{OMZ} (mg m^{-3} d^{-1}) is the remineralization of particulate matter and $E_{O2/P}$ is the elemental ratio of consumed O_2 to P produced through remineralization (170; ref. 2).

Parameter values used in the model are given in Supplementary Table S4.

Further description of model physics, model parameters and constants, and sensitivity analyses are included in the Supplementary Information.

Received 13 January 2010; accepted 30 March 2010; published online 16 May 2010

References

1. Redfield, A. C. in *James Johnstone Memorial Volume* (ed. Daniel, R. J.) 177–192 (Univ. Press Liverpool, 1934).
2. Anderson, L. A. & Sarmiento, J. L. Redfield ratios of remineralization determined by nutrient data-Analysis. *Glob. Biogeochem. Cycles* **8,** 65–80 (1994).
3. Gruber, N. & Sarmiento, J. L. Global patterns of marine nitrogen fixation and denitrification. *Glob. Biogeochem. Cycles* **11,** 235–266 (1997).
4. Moore, J. K., Doney, S. C., Kleypas, J. A., Glover, D. M. & Fung, I. Y. An intermediate complexity marine ecosystem model for the global domain. *Deep-Sea Res. II* **49,** 403–462 (2002).
5. Quigg, A. *et al.* The evolutionary inheritance of elemental stoichiometry in marine phytoplankton. *Nature* **425,** 291–294 (2003).
6. Arrigo, K. R. *et al.* Phytoplankton community structure and the drawdown of nutrients and CO_2 in the Southern Ocean. *Science* **283,** 365–367 (1999).
7. Geider, R. J. & La Roche, J. Redfield revisited: Variability of C:N:P in marine microalgae and its biochemical basis. *Eur. J. Phycol.* **37,** 1–17 (2002).
8. Bertilsson, S., Berglund, O., Karl, D. M. & Chisholm, S. W. Elemental composition of marine *Prochlorococcus* and *Synechococcus*: Implications for the ecological stoichiometry of the sea. *Limnol. Oceanogr.* **48,** 1721–1731 (2003).
9. Klausmeier, C. A., Litchman, E., Daufresne, T. & Levin, S. A. Optimal nitrogen-to-phosphorus stoichiometry of phytoplankton. *Nature* **429,** 171–174 (2004).
10. Deutsch, C., Sarmiento, J. L., Sigman, D. M., Gruber, N. & Dunne, J. P. Spatial coupling of nitrogen inputs and losses in the ocean. *Nature* **445,** 163–167 (2007).
11. Anderson, T. R. & Pondaven, P. Non-Redfield carbon and nitrogen cycling in the Sargasso Sea: Pelagic imbalances and export flux. *Deep-Sea Res. I* **50,** 573–591 (2003).
12. Christian, J. R. Biogeochemical cycling in the oligotrophic ocean: Redfield and non-Redfield models. *Limnol. Oceanogr.* **50,** 646–657 (2005).
13. Chavez, F. P., Buck, K. R., Service, S. K., Newton, J. & Barber, R. T. Phytoplankton variability in the central and eastern tropical Pacific. *Deep-Sea Res. II* **43,** 835–870 (1996).
14. Bruland, K. W., Rue, E. L., Smith, G. J. & DiTullio, G. R. Iron, macronutrients and diatom blooms in the Peru upwelling regime: Brown and blue waters of Peru. *Mar. Chem.* **93,** 81–103 (2005).
15. Dandonneau, Y. *et al.* Seasonal and interannual variability of ocean colour and composition of phytoplankton communities in the North Atlantic, equatorial Pacific and South Pacific. *Deep-Sea Res. II* **51,** 303–318 (2004).
16. Garcia, H. E., Locarnini, R. A., Boyer, T. P. & Anotov, J. I. in *NOAA Atlas NESDIS 64* (ed. Levitus, S.) (US Government Printing Office, 2006).
17. Voss, M., Bombar, D., Loick, N. & Dippner, J. W. Riverine influence on nitrogen fixation in the upwelling region off Vietnam, South China Sea. *Geophys. Res. Lett.* **33,** L07604 (2006).
18. Capone, D. G. *et al.* An extensive bloom of the N_2-fixing cyanobacterium *Trichodesmium erythraeum* in the central Arabian Sea. *Mar. Ecol. Prog. Ser.* **172,** 281–292 (1998).
19. Canfield, D. E. Models of oxic respiration, denitrification and sulfate reduction in zones of coastal upwelling. *Geochim. Cosmochim. Acta* **70,** 5753–5765 (2006).
20. Moore, J. K. & Doney, S. C. Iron availability limits the ocean nitrogen inventory stabilizing feedbacks between marine denitrification and nitrogen fixation. *Glob. Biogeochem. Cycles* **21** (2007).
21. Tagliabue, A., Bopp, L. & Aumont, O. Ocean biogeochemistry exhibits contrasting responses to a large scale reduction in dust deposition. *Biogeosciences* **5,** 11–24 (2008).
22. Glibert, P. M. & Bronk, D. A. Release of dissolved organic nitrogen by marine diazotrophic cyanobacteria, *Trichodesmium* spp. *Appl. Environ. Microbiol.* **60,** 3996–4000 (1994).
23. Yamamoto-Kawai, M., Carmack, E. & McLaughlin, F. Nitrogen balance and Arctic throughflow. *Nature* **443,** 43–43 (2006).
24. Lochte, K., Ducklow, H. W., Fasham, M. J. R. & Stienen, C. Plankton succession and carbon cycling at 47° N 20° W during the JGOFS North-Atlantic bloom experiment. *Deep-Sea Res. II* **40,** 91–114 (1993).
25. Staal, M. *et al.* Nitrogen fixation along a north–south transect in the eastern Atlantic Ocean. *Limnol. Oceanogr.* **52,** 1305–1316 (2007).
26. Richardson, T. L. & Jackson, G. A. Small phytoplankton and carbon export from the surface ocean. *Science* **315,** 838–840 (2007).
27. Schmittner, A. Decline of the marine ecosystem caused by a reduction in the Atlantic overturning circulation. *Nature* **434,** 628–633 (2005).
28. Irwin, A. J. & Oliver, M. J. Are ocean deserts getting larger? *Geophys. Res. Lett.* **36,** L18609 (2009).
29. Codispoti, L. A. *et al.* The oceanic fixed nitrogen and nitrous oxide budgets: Moving targets as we enter the anthropocene? *Sci. Marina* **65,** 85–105 (2001).
30. Paulmier, A., Kriest, I. & Oschlies, A. Stoichiometries of remineralisation and denitrification in global biogeochemical ocean models. *Biogeosciences* **6,** 2539–2566 (2009).

Acknowledgements

We thank G. van Dijken and B. Saenz for help coding the model and L. Thomas for help parameterizing upwelling fluxes. We are also indebted to the members of the Arrigo laboratory and to C. M. Moore for fruitful discussions on nutrient utilization ratios of different phytoplankton and for comments on the manuscript. This work was supported by NSF grant ANT 0732535 and DOE grant DE-FG02-04ER63896 to K.R.A.

Author contributions

All authors contributed equally to this work.

Additional information

The authors declare no competing financial interests. Supplementary information accompanies this paper on www.nature.com/naturegeoscience. Reprints and permissions information is available online at http://npg.nature.com/reprintsandpermissions. Correspondence and requests for materials should be addressed to M.M.M.